Release Mechanisms of Semipolar Solutes from Poly(dimethylsiloxane) Elastomers: Effect of a Hydrophilic Additive

Athanasia I. Panou, Kyriaki G. Papadokostaki, Merope Sanopoulou

Department of Physical Chemistry, Institute of Advanced Materials, Physicochemical Processes, Nanotechnology and Microsystems, National Center for Scientific Research "Demokritos," 15310 Ag. Paraskevi Athens, Greece
Correspondence to: M. Sanopoulou (E-mail: sanopoul@chem.demokritos.gr)

ABSTRACT: The release profiles of three xanthine derivatives from matrices of pure poly(dimethylsiloxane) (PDMS), and the effect of incorporating 10% w/w polyethylene glycol (PEG)−3000 in the matrix are presented. Theobromine (TBR), theophylline (TPL), and caffeine (CAF), although structurally very similar, are characterized by different physicochemical properties. In addition, differential scanning calorimetry and scanning electron microscopy measurements indicate different physical interactions with the polymeric matrices. The observed rates of release from pure PDMS matrices loaded at 0.065 g/g with each one of the drugs increase in the order TBR < TPL < CAF. The same order holds for the corresponding permeabilities derived from the release kinetic data. The slopes of the release curves versus the square root of time were linearly correlated to the square root of calculated solubilities in the polymer, as expected by the Higuchi equation for diffusive transport of solutes of the same diffusivity. The incorporation of 10% w/w PEG in the PDMS matrix accelerates the release rate of each drug, because of the concurrent water uptake induced by the hydrophilic additive. The extent of the corresponding permeability enhancement for theophylline was close to that predicted by the Maxwell equation for a composite two-phase system, consisting of a PDMS continuous phase characterized by a much lower permeability than that of the fully swollen PEG dispersed phase. The corresponding enhancement of permeability was higher for TBR and lower for CAF. Possible reasons for these differences are discussed. © 2014 Wiley Periodicals, Inc. J. Appl. Polym. Sci. **2014**, *131*, 40782.

INTRODUCTION

The suitability of poly(dimethylsiloxane) (PDMS) as a carrier material for long-term release of bioactive substances has been well established several decades ago, with the fabrication and implementation of subdermal contraceptive implants containing steroid hormones.[1,2] These PDMS-based devices, in the form of capsules, rods or covered rods, tested in large groups of women, were capable of continuously releasing in situ steroidal hormones for up to 6 years with varying degrees of rate uniformity depending mainly on the structure of the device. It was also recognized that the permeability of silicone rubber to low-molecular-weight (MW) lipophilic steroids was mainly determined by the solubility of the drug in the polymer.[1,3] Since then, a major part of research efforts on PDMS-based controlled release devices has focused on methods to expand their application in a broader range of pharmaceuticals such as hydrophilic drugs and proteins. Other, nonsteroidal small MW drugs of varying polarity have also been found to be effectively
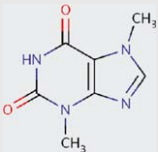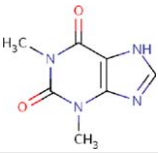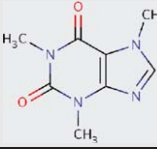
released by diffusive transport through PDMS,[4–8] including semipolar water-soluble ones such as metronidazol.[9,10] However, the effective release of water-soluble macromolecules such as the proteins interferon[11,12] and bovine serum albumin[13,14] requires the modification of the release mechanism by addition of hydrophilic excipients in the PDMS matrix. This strategy has also been applied to other solutes ranging from water-insoluble ones such as ivermectin[15] to water-soluble ones such as nicotine.[16] In relation to chemically induced hydrophilicity in PDMS, by covalent grafting or copolymerization, the addition of hydrophilic excipients has the advantage of relatively easy laboratory crosslinking of prepolymers, or of commercially available medical-grade formulations, at room temperature.

In general, hydrophilic additives, such as sugars[11,13,17] and polyethylene glycols[16–20] promote the water uptake and facilitate the release of the drug through water-filled areas in the hydrophobic matrix. Additives of mild osmotic action promote the rate of release only moderately if present at low contents, as the

---

Additional Supporting Information may be found in the online version of this article.

Table I. Structure and Properties of Xanthine Derivatives

Drug	Structure	Aqueous solubility[a], c_{NS}^o (mg/cm^3), 37°C	T_m[b] (°C)	ΔH_o[b] (J/g)
Theobromine (TBR)		0.72	351.6	223.1
Theophylline (TPL)		11.81	274.1	162.5
Caffeine (CAF)		37.47	238.4	110.5

[a] Taken from Ref. 29.
[b] Determined in this work.

swollen areas are isolated. At high contents, they are considered to eventually create a continuous network of channels, through which release of the drug is accelerated. This process is further intensified if the additive is of high osmotic pressure, such as inorganic salts in the form of particles, resulting in microscopic cracks due to the osmotically induced water. The cracks eventually form an interconnecting network filled with water, leading to intense acceleration of the release process and strong deviations from diffusion-controlled release kinetics.[21,22] These complex transport mechanisms, which can also be initiated by the drug itself, if it exerts an osmotic action and/or is present at high loads,[23,24] have been studied in detail.[25–27] However, systematic investigations on the parameters affecting the release acceleration induced by hydrophilic additives of mild osmotic action are more rare.

Accordingly, in view of the interest in PDMS-based controlled release devices suitable for bioactive substances of varying physico-chemical characteristics, we have studied the release of three xanthine derivatives from matrices of PDMS or PDMS modified by the addition of 10% w/w PEG of MW 3000. The xanthine derivatives were chosen as to present a rather wide range of solubilities in water, but a narrow range in MW, in an effort to isolate and study the solubility-related effects on the release mechanisms.

EXPERIMENTAL

Materials
PDMS, type RTV 615 was kindly supplied by Momentive (USA) in a two-component kit (part A and part B). According to the MSDS of RTV615, part A contains a vinylpolydimethylsiloxane prepolymer, and part B (the crosslinking agent) contains a mixture of polydimethylsiloxane terminated with vinyl and hydrogen groups. Curing of vinyl-terminated polysiloxanes occurs via an addition reaction between vinyl and hydrosilane groups in the presence of a Pt catalyst[28] or other metal catalysts. Polyethylene glycol (PEG) of MW = 3000 g/mol and of density

$d = 1.21$ g/cm^3 was purchased from Merck (Germany). Toluene, chloroform, and dichloromethane (Merck) were all of analytical reagent grade.

Three xanthine derivatives were used: theobromine base anhydrous (TBR), $C_7H_8N_4O_2$ (Serva, Germany) with MW = 180.2 g/mol and $d = 1.61$ g/cm^3, theophylline anhydrous (TPL), $C_7H_8N_4O_2$ (Acros Organics, Belgium) with MW = 180.2 g/mol and $d = 1.47$ g/cm^3, and caffeine anhydrous (CAF), $C_8H_{10}N_4O_2$ (Fluka, Germany) with MW = 194.2 g/mol and $d = 1.23$ g/cm^3. As it can be seen in Table I, only small differences between the structures of these molecules affect considerably their physical properties, with TBR exhibiting the lowest aqueous solubility and the highest melting temperature and CAF being the most water soluble with the lowest melting temperature.

Preparation of Matrices
Loaded pure PDMS matrices were prepared by adding the appropriate amount of drug to the RTV prepolymer mixture, consisting of parts A and B at a 10 : 1 w/w ratio, before curing. Typically, ~5.5 g of A and B mixture was first mechanically stirred for 1 h and then ~0.385 g of drug and 1 mL of dichloromethane were added, and the viscous fluid was further stirred for $1/2$ h before casting on a poly(propylene)-coated glass plate by means of a blade with an adjustable gap separation. The casted mixture was cured at 100°C for 1 h. For the PDMS–PEG matrices containing 10% w/w PEG, the same procedure was followed, with the only difference that the 1 mL of dichloromethane added contained ~0.61 g of dissolved PEG. The thicknesses, L, of the cured matrices, measured by means of a micrometer reading to 1 μm, at five different points of the matrix area, were in the range 90–200 μm. The drug load was approximately the same in all cases, ranging from 0.059 to 0.065 g/g.

SEM and DSC Studies
Fractured cross sections of the samples were prepared by freezing in liquid nitrogen for several minutes and then immediately
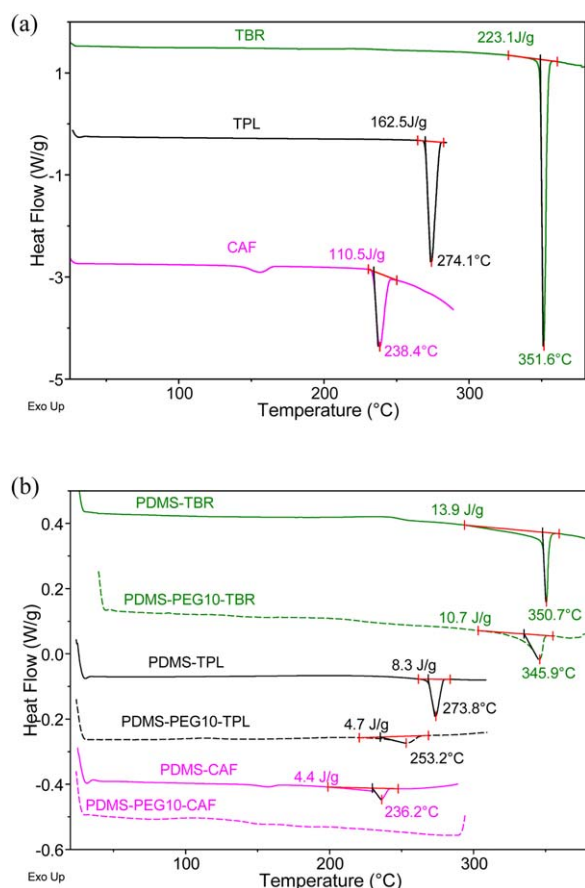
Figure 1. (a) DSC thermographs for pure drugs. (b) Representative DSC thermographs of PDMS and PDMS–PEG matrices loaded to (g/g): 0.065 (PDMS) and 0.059 (PDMS–PEG). The heating rate was 5°C/min. The DSC thermographs have been displaced vertically for clarity. [Color figure can be viewed in the online issue, which is available at wileyonlinelibrary. com.]

breaking the frozen sample with a scalpel. The samples were coated with platinum and characterized using a JEOL 7401F field emission scanning electron microscopy (FESEM).

A 2920 modulated differential scanning calorimeter–MDSC (TA Instruments) was used to perform heating runs on pure drug samples of about 5 mg, from ambient temperature up to the melting temperature of each drug with a nonmodulated heating rate of 5°C/min, in a nitrogen atmosphere. The same procedure was followed for 10 mg samples of drug-loaded PDMS and PDMS–PEG matrices.

Release Experiments
All release experiments were performed in degassed deionized water at 37°C ± 0.2°C in samples of 3 × 3 cm² lateral dimensions. For TPL- and CAF-loaded samples, a dissolution system (DT-810, Jasco, Japan) coupled with an automatic fraction collector and sampler (FC-812AS, Jasco) and a UV/Vis spectrophotometer (V-630, Jasco) was used. Samples were suspended by custom-made holders rotating at 100 rpm in dissolution vessels. At suitable time intervals 5 mL samples were automatically collected. TPL and CAF release were monitored at 271 and 272 nm, respectively. The sample solution, after been measured, was

drained and appropriate corrections were made for compensating the volume loss. Because of the protracted time period needed for the release of TBR, a home-made apparatus was used consisting of a bath thermostated at 37°C ± 0.2°C. Matrices were mounted on stirring rods rotating at 100 rpm in deionized water vessels and TBR was monitored at 273 nm.

RESULTS AND DISCUSSION

Characterization of Matrices
Information on the physical state of the drugs within the polymeric matrices was derived from DSC and SEM studies. In DSC measurements (Figure 1) the samples were heated at 5°C/min up to the melting temperature of each pure drug and the melting endotherm produced by the dispersed crystalline drug upon heating was recorded and used to determine the heat of melting ΔH, expressed in J/g matrix. The ratio of ΔH over the heat of melting of pure 100% crystalline drug, ΔH_o (J/g crystalline drug) (Table I), represents the amount of crystalline drug in the matrix at the recorded melting temperature. The $\Delta H/\Delta H_o$ values in pure PDMS were increasing in the order CAF < TPL < TBR (Table II). Upon inclusion of the drugs in the PDMS–PEG matrices, $\Delta H/\Delta H_o$ decreased slightly in the case of TBR and to a greater extent in the case of TPL, whereas the melting endotherm of CAF was not detectable. When compared with the thermograms of the pure crystalline drugs, the sharpness of the melting endotherm and the T_m values were not materially affected upon inclusion of the drugs in pure PDMS matrices owing to the limited miscibility between polar PDMS and the semipolar drugs. However, the endotherm became broader in PDMS–PEG matrices for both TBR and TPL (Figure 1b), and moreover, T_m was lowered by ~5°C for TBR and ~20°C for TPL.

It should be noted that the amount of noncrystalline drug (drug load − $\Delta H/\Delta H_o$) determined at the melting temperature of each drug is not a reliable estimate of the drug's solubility in the polymer matrix at 37°C, because the drug may partially dissolve with increasing temperature during the DSC heating run.[30,31] However, the observed trends in $\Delta H/\Delta H_o$ values and in melting point depression point to CAF and to a lesser extend to TPL, as the drugs (i) with stronger physical interactions and miscibility with PDMS[32,33] and (ii) more favorably affected, in terms of solubilization, by the presence of PEG in the matrix.

In line with these observations was the qualitative examination of the fractured surfaces of drug-loaded PDMS matrices. Drug aggregates are clearly visible in the TBR–PDMS matrix [Figure 2(a)], whereas the TPL–PDMS one has a more smooth

Table II. Amount of Crystalline Drug in the Matrix, as Recorded in DSC Heating Runs

| Drug | $\Delta H/\Delta H_o$ (g crystalline drug/g matrix) | |
	PDMS	PDMS–PEG10
TBR	0.062	0.048
TPL	0.055 ± 0.003	0.031 ± 0.006
CAF	0.043 ± 0.005	0
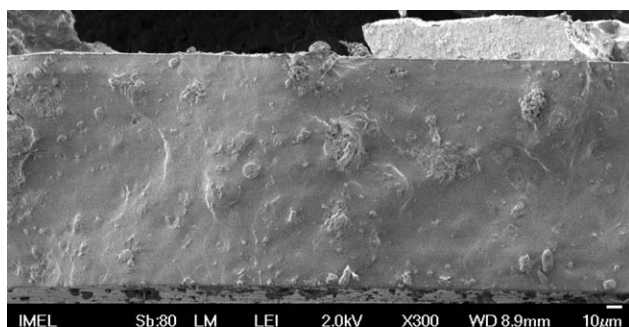
Figure 2. SEM images of fractured cross sections of (a) TBR–PDMS matrix and (b) TPL–PDMS matrix, both loaded to 0.065 g/g.

cross section [Figure 2(b)]. Similar to TPL–PDMS images, were those of CAF–PDMS ones.

Neat (unloaded) PDMS–PEG matrices were shown to present a two-phase morphology with spherical PEG-phase domains (diameters of 4–8 μm) evenly distributed in the continuous PDMS phase (Figure 1 in Ref. 34). In the case of TPL–PDMS–PEG matrices, spherical PEG moieties of approximately the same size as those in the pure PDMS–PEG are discernible, along with few larger TPL aggregates [Figure 3(a)]. In contrast, the spherical domains in the CAF–PDMS–PEG cross section [Figure 3(b)] are more and of smaller size, indicating that the presence of CAF alters the dispersion of PEG in the PDMS matrix.

Calculation of Partition Coefficients and Solubilities in PDMS

As all three solutes are of similar molecular volumes, provided that transport is diffusive, any differences in their permeabilities through PDMS should result mainly from differences in their corresponding partition coefficients, K_N, between the polymer and the external aqueous phase

$$K_N = \frac{C_{NS}^o}{c_{NS}^o}, \tag{1}$$

where C_{NS}^o is the drug's solubility in the PDMS matrix and c_{NS}^o is the drug's solubility in the external medium (water).

Estimation of the K_N values in PDMS was based on a correlation of octanol–water, and PDMS–water, partition coefficients of the solutes:[35,36]

$$\log K_N = 1.52 \log K_{o/w} - 3.37, \tag{2}$$

where $K_{o/w}$ is the octanol–water partition coefficient of the solute. Equation (2) was derived from a series of low MW solutes of $\log K_{o/w}$ values in the range 1–4 (i.e., representing a 1000-fold increase in lipophilicity) and experimental K_N values, determined at 37°C, covering more than five orders of magnitude range. The validity of eq. (2) was further checked here (Figure 4), by experimental literature data on K_N values of (i) various, mostly steroidal, solutes in PDMS,[37] (ii) steroidal and more polar molecules in PDMS fluid (silicone oil),[4,38] and (iii) a series of alkyl p-amino benzoates in PDMS fluid.[39] Detailed data used for constructing the plot of Figure 4 can be found in Supporting Information. The results shown in Figure 4 provide adequate evidence to justify the use of eq. (2) for less lipophilic
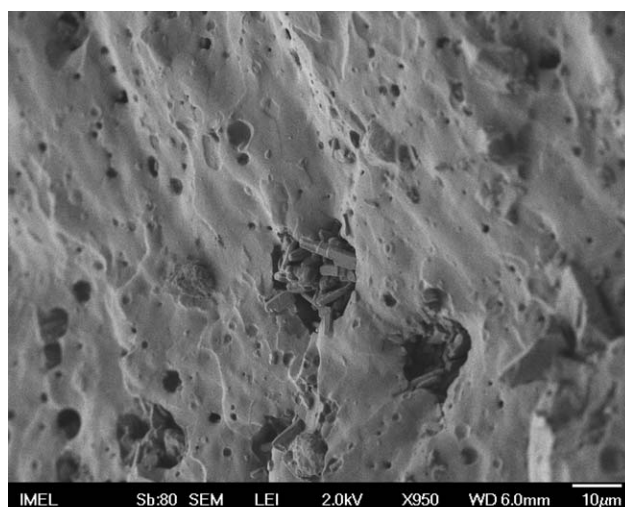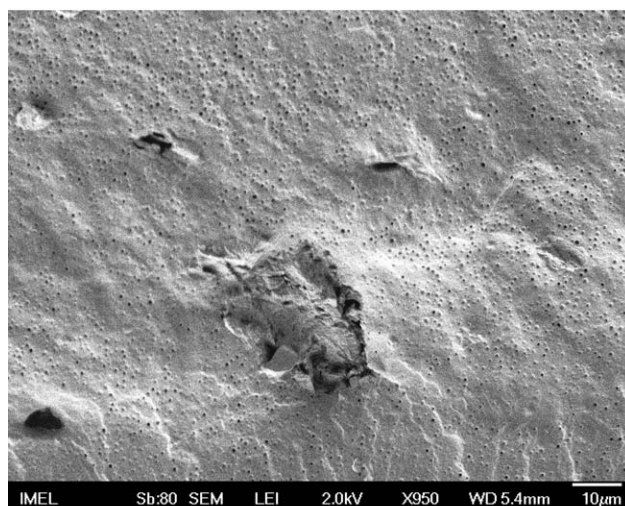
Figure 3. SEM images of fractured cross sections of (a) TPL–PDMS–PEG matrix and (b) CAF–PDMS–PEG matrix, both loaded to 0.059 g/g.
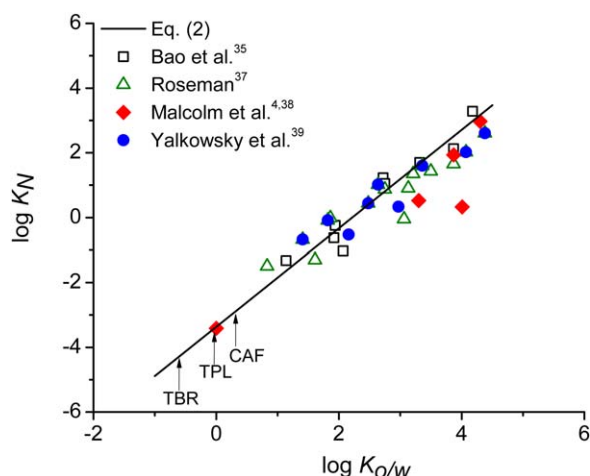
Figure 4. Correlation of solute partition coefficients in octanol–water ($K_{o/w}$) and PDMS–water (K_N). Experimental literature data (points) and predictions of eq. (2) (line). Data of Bao et al.,[35] Roseman,[37] and Yalkowsky et al.[39] were directly given in K_N values. Malcolm et al.[4,38] provide solubilities in PDMS fluid, which were used here, in conjunction with aqueous solubilities, to calculate K_N. More information is given in Supporting Information. The calculated K_N values for TBR, TPL, and CAF, on the basis of eq. (2), are indicated by arrows. [Color figure can be viewed in the online issue, which is available at wileyonlinelibrary.com.]

drugs than those originally used for its derivation. Accordingly, K_N values of TBR, TPL, and CAF were estimated from eq. (2) using the calculated $\log K_{o/w}$ values of -0.67, -0.05, and 0.26, respectively.[40] The K_N value for TPL was 4×10^{-4}, i.e., similar to the experimental value for metronidazole, a solute of similar lipophilicity and aqueous solubility.[4] The K_N value for CAF was higher (1.02×10^{-3}) and that of TBR one order of magnitude lower (4×10^{-5}). The K_N values in conjunction with the aqueous solubilities of the drugs (Table I) were then used to estimate each drug's solubility in the PDMS matrix, C_{NS}^o, from eq. (1). These values, being 2.9×10^{-8}, 4.2×10^{-6}, and 3.9×10^{-5} g/cm³ for TBR, TPL, and CAF, respectively, are well below the initial drug concentration C_{N0} ($\sim 6.5 \times 10^{-2}$ g/cm³) used in this work. We finally note that the order of decreasing solubilities correlates with the order of increasing amount of crystalline drug ($\Delta H / \Delta H_o$) as determined by DSC (Table II).

Release Experiments

Release Kinetics from Pure PDMS Matrices. The release kinetics of the three drugs from pure PDMS matrices are shown in Figure 5 as fractional amount of drug released $Q_{Nt}/Q_{N\infty}$ on a $t^{1/2}/L$ scale. Release rates increase in the order TBR < TPL < CAF. On a non-normalized time scale, 80% of CAF or TPL was released at ~ 0.5 and ~ 2 days, respectively, whereas only 60% of TBR was released at 100 days. All three drugs have similar MW, $\log K_{o/w}$ values lower than 1, and varying solubilities in water. However, even the more soluble CAF did not provoke any water uptake in the PDMS matrix during the release process in pure water. As shown in Figure 5, except for a slight deviation at the early stages of the process, $t^{1/2}$ kinetics is observed in all cases. Accordingly, diffusive transport through the PDMS matrix is assumed and the results of

Figure 5 can be quantified and analyzed on the basis of Higuchi kinetics,[41] applicable to systems where the drug concentration, C_{N0}, is well above the drug's solubility in the matrix C_{NS}^o,

$$\frac{Q_{Nt}}{Q_{N\infty}} \cong 2\sqrt{\frac{2D_N C_{NS}^o t}{L^2 C_{N0}}} \tag{3a}$$

$$\cong 2\sqrt{\frac{2P_N c_{NS}^o t}{L^2 C_{N0}}}, \tag{3b}$$

where D_N is the diffusion coefficient of the drug in the matrix and P_N is the permeability coefficient of the drug. The expression of $Q_{Nt}/Q_{N\infty}$ in terms of P_N [(eq. (3b)] is derived on the basis of the definition of P_N as the product of the diffusion coefficient D_N and the partition coefficient K_N. Equation (3) is valid under conditions of fast dissolution of dispersed solute in relation to the diffusion of the dissolved solute.

The diffusion coefficients of the three drugs are not expected to differ substantially, as they are of similar molar volume. Thus, on the basis of eq. (3a), for the same drug concentrations C_{N0} studied here, the observed differences in release rates should mainly reflect their different solubilities in the polymer, C_{NS}^o. In particular, a linear relation between the slopes of the linear parts of the curves in Figure 5 and the square root of C_{NS}^o is predicted by eq. (3a). Figure 6 shows the slopes of the $Q_{Nt}/Q_{N\infty}$ vs. $(t^{1/2}/L)$ plots of Figure 5 vs. the square root of the C_{NS}^o values, calculated in the previous section. A satisfactory linear correlation with $R^2 > 0.99$ is obtained in Figure 6. Moreover, on the basis of eq. (3a), the slope of the least-square fit gives a value of $D_N = 9.4 \times 10^{-7}$ cm²/s. This value compares well with reported diffusivities in PDMS ranging from 5.8×10^{-7} to 1.5×10^{-6} cm²/s for solutes of $135 < MW < 400$.[37] We also note that the same analysis of the release data of three progesterone-type steroids of $316 < MW < 386$ and varying solubilities in PDMS was performed by Roseman[3] and the D_N value derived from the linear correlation on the basis of eq. (3a) was 5.1×10^{-7} cm²/s. Thus, the results of Figure 5 indicate that the solubility-controlled transport of small lipophilic steroids in
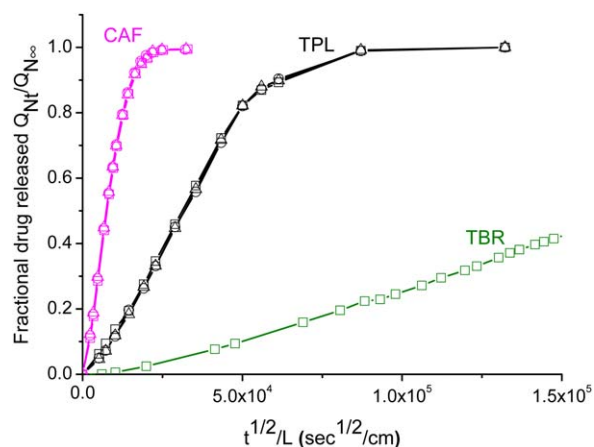

Figure 5. Release kinetics of TBR, TPL, and CAF from PDMS matrices at 37°C. Initial drug loads are 0.065g/g. Matrix thickness L (μm): 141 (TBR); 85–88 (TPL); and 125–128 (CAF). [Color figure can be viewed in the online issue, which is available at wileyonlinelibrary.com.]
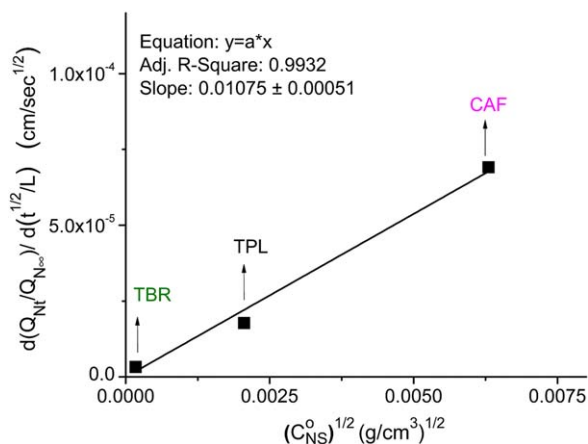
Figure 6. Correlation of the slope of release kinetic curves from pure PDMS, $d(Q_{Nt}/Q_{N\infty})/d(t^{1/2}/L)$, with the square root of calculated solubilities in PDMS, C_{NS}^o. [Color figure can be viewed in the online issue, which is available at wileyonlinelibrary.com.]

PDMS is also applicable for relatively hydrophilic (semipolar) small molecules.

Permeability coefficients, P_N, were derived from the slope of the linear parts of the release curves of Figure 5, on the basis of eq. (3b), with the use of the aqueous solubilities at 37°C shown in Table I. P_N values were increasing in the order of TBR < TPL < CAF (Table III), being 1.1×10^{-10} cm²/s for TBR, 2×10^{-10} cm²/s for TPL, and 1.04×10^{-9} cm²/s for CAF. These values compare reasonably well with literature data on small MW drugs of semipolar nature in PDMS. For example, reported P_N values range (i) from 2.2×10^{-9} to 6×10^{-9} cm²/s for CAF[42,43] and (ii) from 5.5×10^{-9} to 2×10^{-8} cm²/s for the moderately water-soluble hydrocortisone of MW = 362.[37,44] On the other hand, P_N values of lipophilic steroids, such as progesterone, are at least three orders of magnitude higher, varying from 10^{-6} to 3×10^{-5} cm²/s.[37,44]

Effect of PEG on Release Rates. Release kinetics from PDMS–PEG matrices are shown in Figure 7(a–c) for TBR, TPL, and CAF, respectively. In the same plots, the corresponding data of Figure 5, pertaining to the release kinetics from pure PDMS, are also included. In all cases, the release rate increases upon inclusion of PEG in the matrix. The dashed line in each plot represents water uptake kinetics in neat PDMS–PEG films at 25°C, taken from Panou et al.[34] Our previous work on water uptake measurements on neat (unloaded) PDMS–PEG films showed that (i) the presence of 10% PEG in PDMS results in ~0.67 g/g of water in the matrix at equilibrium, and (ii) once equilibrium is reached, the weight of the films remains practically constant for more than 40 days, indicating that PEG was not leached out of the matrix during this period.[34] In comparison, the total amount of TBR, exhibiting the lowest rates, is released from the PDMS–PEG matrices at ~50 days, i.e., in a time period where leaching of PEG is not expected to occur, and thus interfere with, the release process. Gravimetric measurements at the end of the release experiments confirmed this conclusion. Thus, the observed enhancement of release rates upon inclusion of PEG

in the matrix is attributed to the PEG-induced water penetration during the release process. (As already mentioned, during release from the pure PDMS matrices no imbibition of water was observed). The observed enhancement of release rates is unlikely to be produced by extensive crack growth of the PDMS polymeric walls surrounding the swollen PEG inclusions, as the osmotic pressure of PEG is relatively low (when compared with highly soluble inorganic salts used also as additives in PDMS[21,22]) and results in only moderate water uptake by the PDMS–PEG matrices. Thus, assuming that both PEG leaching and extensive crack growth phenomena are absent during the release process, the effect of PEG inclusions on the permeability of the matrix can be compared with the predictions of the Maxwell model for a two-phase system. According to this approach, the permeability of a composite material (denoted as P_{NC}), consisting of a continuous phase N of permeability coefficient P_N (PDMS here) and a dispersed phase A of permeability coefficient P_A (water-swollen PEG inclusions here) is given by[45]

$$\frac{P_{NC}}{P_N} = 1 + 3v_A \left(\frac{\alpha+2}{\alpha-1} - v_A \right)^{-1}, \qquad (4)$$

where $\alpha = P_A/P_N$ and v_A is the volume fraction of the dispersed phase.

Assuming that all the water imbibed by the composite PDMS–PEG matrix (~0.67 g H₂O/g) resides in the PEG phase, the volume fraction of the swollen PEG phase v_A is ~0.45. On the basis of eq. (4), the calculated enhancement of permeability P_{NC}/P_N at $v_A = 0.45$ is 3.45, 3.44, and 3.32 for $\alpha (= P_A/P_N)$ infinite, 1000, and 100, respectively. To compare our results with the predictions of eq. (4), we derived values of effective permeability coefficients (denoted as P_{NC} for the PDMS–PEG matrices) from the plots of Figure 7, as described in the previous section. The results are shown in Table III, together with the ratios P_{NC}/P_N for each drug. The value $P_{NC}/P_N = 2.9$ for TPL is the one closer to the predictions of eq. (4) for high values of α. Values of $\alpha \geq 100$ are reasonable estimates for the systems studied here, taking into account that both the partition coefficient and the diffusivity of the drugs are expected to be significantly higher in the swollen PEG phase when compared with the PDMS one.

The higher (lower) experimental P_{NC}/P_N values for TBR (CAF) when compared with the predictions of eq. (4) may arise from deviations of the experimental systems from the idealized conditions under which eq. (4) is strictly valid. Thus, we note that the rate of water uptake in the PDMS–PEG matrix (blue lines in Figure 7) is fast compared to the release of TPL and especially of TBR, but lags behind the release of CAF. Thus, the

Table III. Permeability Coefficients Derived from Release Kinetics on the Basis of eq. (3a)

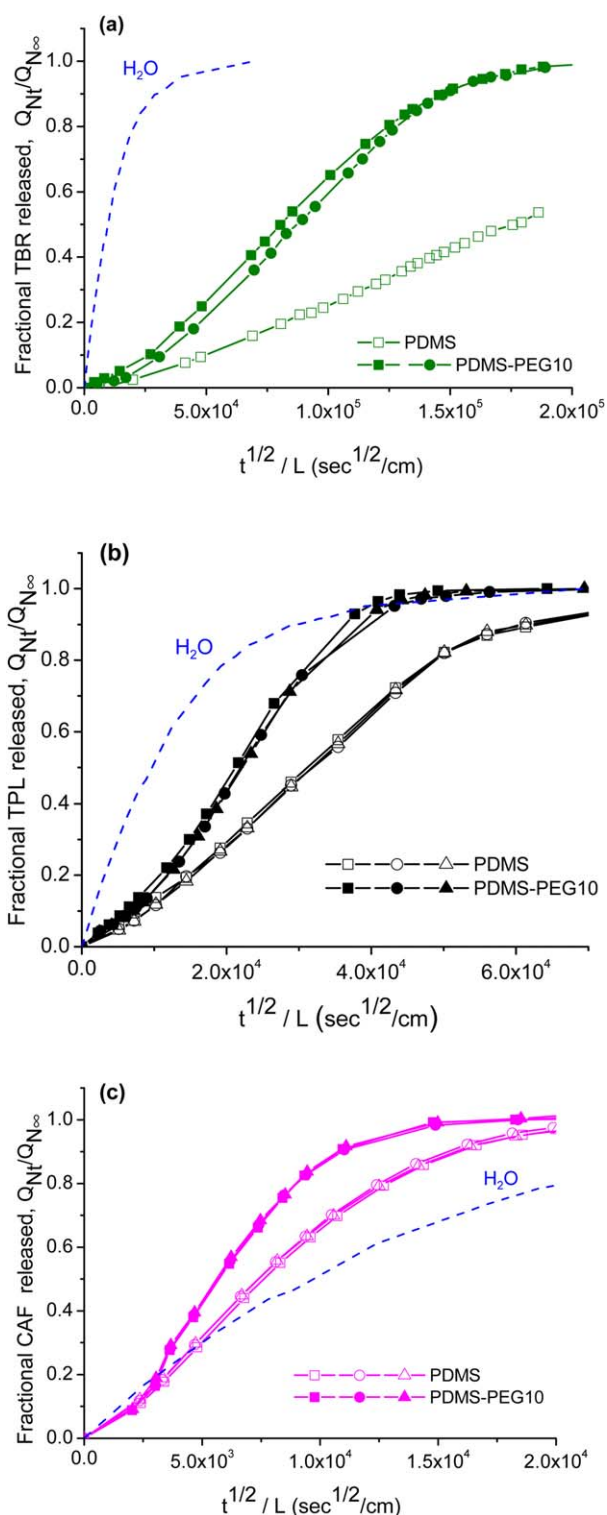| Drug	$P_N \times 10^{10}$ (cm²/s) in PDMS	$P_{NC} \times 10^{10}$ (cm²/s) in PDMS-PEG	P_{NC}/P_N
TBR	1.2	5.8 ± 0.2	4.9
TPL	2.2 ± 0.1	6.4 ± 0.4	2.9
CAF	10.4 ± 0.8	17.9 ± 2.2	1.7

Figure 7. Effect of PEG on release rates of (a) TBR, (b) TPL, and (c) CAF at 37°C. Open points denote release from pure PDMS matrices and full points release from PDMS–PEG matrices containing 10% w/w PEG. The dashed line in each plot represents water uptake kinetics in neat PDMS–PEG films at 25°C, taken from Ref. 34 (data of Figure 6a therein). PDMS–PEG matrices were loaded to 0.059 g/g and their thickness ranged from 99 to 105 μm for TBR, 170 to 185 μm for TPL, and 145 to 150 μm for CAF. [Color figure can be viewed in the online issue, which is available at wileyonlinelibrary.com.]

PEG phase may not be fully swollen in the later case, i.e., in terms of eq. (4) the operating value of ν_A may be less than the value of 0.45 used in the above calculations. In other words, the rate of CAF release maybe partly controlled by the rate of water uptake. Other parameters may also affect the permeability of the drugs in the two phases of the composites, as for example, different internal morphologies for the different drugs (as indicated by the SEM images of Figure 3), or the different tendencies of the various xanthine derivatives to self-association or to hydrate formation in aqueous solutions.[46,47]

CONCLUSIONS

The three xanthine derivatives studied here, although structurally very similar, exhibit differences in physicochemical properties that are crucial for their release profiles from PDMS-based polymeric matrices. In relation to the release mechanism from pure PDMS matrices, it was shown that it is controlled by diffusive transport, as in the case of more lipophilic micromolecular substances. This conclusion was based on the linear correlation of the slopes of the release curves ($Q_{Nt}/Q_{N\infty}$ vs. $t^{1/2}/L$) of the three drugs with the square root of the corresponding calculated solubilities in PDMS, as predicted by the Higuchi equation. Another point that may be useful in relevant studies is that a previously proposed equation, on the prediction of PDMS–water partition coefficients of solutes from their octanol–water partition coefficients, was further validated here against experimental data found in different literature sources.

The incorporation (at 10% w/w) of a hydrophilic additive of mild osmotic action (PEG) in the PDMS matrix resulted in enhancement of the release rates due to the ensuing water uptake. It was shown that the corresponding moderate enhancement of the permeability of the matrix, expressed as ratio of the permeability coefficients in PDMS–PEG and PDMS, P_{NC}/P_N, is anticipated by the predictions of the Maxwell model for a two-phase system, consisting of a PDMS continuous phase characterized by a much lower permeability than that of the fully swollen PEG dispersed phase. The theophylline P_{NC}/P_N value was the one closer to the theoretical values. The observed higher (lower) experimental P_{NC}/P_N values for TBR (CAF) may arise from deviations of the experimental systems from the idealized conditions of the model systems, as for example, caffeine release rate partly controlled by the rate of water uptake in the composite matrix.

REFERENCES

1. Nash, H. A.; Robertson, D. N.; Moo Young, A. J.; Atkinson, L. E. *Contraception* **1978**, *18*, 367.

2. Robertson, D. N.; Sivin, I.; Nash, H. A.; Braun, J.; Dinh, J. *Contraception* **1983**, *27*, 483.

3. Roseman, T. J. *J. Pharm. Sci.* **1972**, *61*, 46.

4. Malcolm, K.; Woolfson, D.; Russell, J.; Tallon, P.; McAuley, L.; Craig, D. *J. Control. Release* **2003**, *90*, 217.

5. Schierholz, J. M. *Biomaterials* **2007**, *18*, 635.

6. Snorradottir, B. S.; Gudnason, P. I.; Scheving, R.; Thorsteinsson, F.; Masson, M. *Pharmazie* **2009**, *64*, 19.

7. Dash, A. K.; Suryanarayanan, R. *Pharm. Res.* **1992**, *9*, 993.

8. Fetherston, S. M.; Boyd, P.; McCoy, C. F.; McBride, M. C.; Edwards, K.-L.; Ampofo, S.; Malcolm, R. K. *Eur. J. Pharm. Sci.* **2013**, *48*, 406.

9. Malcolm, R. K.; McCullagh, S. D.; Woolfson, A. D.; Gorman, S. P.; Jones, D. S.; Cuddy, J. *J. Control. Release* **2004**, *97*, 313.

10. Vasilakos, S. P.; Tarantili, P. A. *J. Biomed. Mater. Res. B* **2012**, *100*, 1899.

11. Kajihara, M.; Sugie, T.; Hojo, T.; Mizuno, M.; Tamura, N.; Sano, A.; Fujioka, K.; Kashiwazaki, Y.; Yamaoka, T.; Sugawara, S.; Urabe, Y. *J. Control. Release* **2000**, *66*, 49.

12. Kajihara, M.; Sugie, T.; Maeda, H.; Sano, A.; Fujioka, K.; Urabe, Y.; Tanihara, M.; Imanishi, Y. *Chem. Pharm. Bull.* **2003**, *51*, 15.

13. Morrow, R. J.; Woolfson, A. D.; Donnelly, L.; Curran, R.; Andrews, G.; Katinger, D.; Malcolm, R. K. *Eur. J. Pharm. Biopharm.* **2011**, *77*, 3.

14. McConville, C.; Andrews, G. P.; Woolfson, A. D.; Malcolm, R. K. *J. Appl. Polym. Sci.* **2012**, *124*, 805.

15. Maeda, H.; Brandon, M.; Sano, A. *Int. J. Pharm.* **2003**, *261*, 9.

16. Brook, M. A.; Holloway, A. C.; Ng, K. K.; Hrynyka, M.; Moore, C.; Lall, R. *Int. J. Pharm.* **2008**, *358*, 121.

17. Maeda, H.; Ohashi, E.; Sano, A.; Kawasaki, H.; Kurosaki, Y. *J. Control. Release* **2003**, *90*, 59.

18. Gao, Z.; Schulze Nahrup, J.; Mark, J. E.; Sakr, A. *J. Appl. Polym. Sci.* **2005**, *96*, 494.

19. Ratner, B.; Kwok, C.; Walline, K.; Johnston, E.; Miller, R. J. U.S. Patent No. US 2006/0204537 A1, **2006**.

20. Carelli, V.; Di Colo, G.; Nannipieri, E.; Serafini, M. F. *J. Control. Release* **1995**, *33*, 153.

21. Carelli, V.; Di Colo, G.; Guerrini, C.; Nannipieri, E. *Int. J. Pharm.* **1989**, *50*, 181.

22. Soulas, D. N.; Papadokostaki, K. G. *Int. J. Pharm.* **2011**, *408*, 120.

23. Maeda, M.; Moriuchi, S.; Sano, A.; Yoshimine, T. *J. Control. Release* **2002**, *84*, 15.

24. Soulas, D. N.; Papadokostaki, K. G. *J. Appl. Polym. Sci.* **2011**, *120*, 821.

25. Schirrer, R.; Thepin, P.; Torres, G. *J. Mater. Sci.* **1992**, *27*, 3424.

26. Amsden, B. *J. Control. Release* **2003**, *93*, 249.

27. Soulas, D. N.; Sanopoulou, M.; Papadokostaki, K. G. *J. Appl. Polym. Sci.* **2009**, *113*, 936.

28. Stafie, N.; Stamatialis, D. F.; Wessling, M. *Sep. Purif. Technol.* **2005**, *45*, 220.

29. Sriamornsak, P.; Kennedy, R. A. *Eur. J. Pharm. Sci.* **2007**, *32*, 231.

30. Bikiaris, D.; Papageorgiou, G. Z.; Stergiou, A.; Pavlidou, E.; Karavas, E.; Kanaze, F.; Georgarakis, M. *Thermochim. Acta* **2005**, *439*, 58.

31. Qi, S.; Belton, P.; Nollenberger, K.; Clayden, N.; Reading, M.; Craig, D. Q. M. *Pharm. Res.* **2010**, *27*, 1869.

32. Marsac, P. J.; Shamblin, S. L.; Taylor, L. S. *Pharm. Res.* **2006**, *23*, 2417.

33. Loreti, G.; Maroni, A.; Del Curto, M. D.; Melocchi, A.; Gazzaniga, A.; Zema, L. *Eur. J. Pharm. Sci.* **2014**, *52*, 77.

34. Panou, A. I.; Papadokostaki, K. G.; Tarantili, P. A.; Sanopoulou, M. *Eur. Polym. J.* **2013**, *49*, 1803.

35. Bao, Y. T.; Samuel, N. K. P.; Pitt, C. G. *J. Polym. Sci. Part C: Polym. Lett.* **1988**, *26*, 41.

36. Pitt, C. G.; Bao, Y. T.; Andrady, A. L.; Samuel, N. K. P. *Int. J. Pharm.* **1988**, *45*, 1.

37. Roseman, T. J. In Controlled Release Technologies: Methods, Theory and Applications; Kydonieus, A. F., Ed.; CRC Press, Inc.: Boca Raton, FL, **1980**; Chapter 2, p 21.

38. Malcolm, R. K.; Woolfson, A. D.; Russell, J.; Andrews, C. *J. Control. Release* **2003**, *91*, 355.

39. Yalkowsky, S. H.; Flynn, G. L.; Slunick, T. G. *J. Pharm. Sci.* **1972**, *61*, 852.

40. Biagi, G. L.; Guerra, M. C.; Barbaro, A. M.; Barbieri, S.; Recanatini, M.; Borea, P. A.; Pietrogrande, M. C. *J. Chromatogr.* **1990**, *498*, 179.

41. Higuchi, T. *J. Pharm. Sci.* **1961**, *50*, 874.

42. Binks, B. P.; Fletcher, P. D. I.; Johnson, A. J.; Elliott, R. P. *Phys. Chem. Chem. Phys.* **2012**, *14*, 15525.

43. Dias, M.; Farinha, A.; Faustino, E.; Hadgraft, J.; Pais, J.; Toscano, C. *Int. J. Pharm.* **1999**, *182*, 41.

44. Kratochvil, P.; Benagiano, G.; Kincl, F. A. *Steroids* **1970**, *15*, 505.

45. Petropoulos, J. H. *J. Polym. Sci. Polym. Phys. Ed.* **1985**, *23*, 1309.

46. Guttman, D.; Higuchi, T. *J. Am. Pharm. Assoc. Sci.* **1957**, *46*, 4.

47. Shefter, E.; Higuchi, T. *J. Pharm. Sci.* **1963**, *52*, 781.